$$[^3CT] = C_0/(\lambda_1 - \lambda_2)[(\lambda_2 - k_d)\exp(-\lambda_2 t) + (k_d - \lambda_1)\exp(-\lambda_1 t)]$$

$$\lambda_2 = [(k_c + k_d) + [(k_c + k_d)^2 + 4k_2k_{-2}]^{1/2}/2] > 0$$

$$\lambda_1 = [(k_c + k_d) - [(k_c + k_d)^2 + 4k_2k_{-2}]^{1/2}/2] > 0 \quad (12)$$

$$k_d - \lambda_1 > 0 \qquad k_d = k_{-2} + k_3$$

$$\lambda_2 - k_d > 0 \qquad k_c = k_1 + k_2$$

In the general case, the molecules decay with a biexponential decay. One rate reflects the extra pathway of initial population of the ^{3}MC state before significant electron back-transfer occurs. The other rate reflects the equilibrium decay of the system. A significant simplification can be made if it is assumed that $k_d >> k_c$. This is a reasonable assumption given that (1) clear experimental evidence for the ^{3}MC state has not been demonstrated for $[Ru(bpy)_3]^{2+}$ via techniques such as flash photolysis,[39] indicating k_3 must at least be larger and possibly much larger than k_1 and that (2) the electron-back-transfer rate, k_{-2}, should be larger than the forward, k_2, since the reaction coordinate is the same and the transfer is now exothermic. For $k_d >> k_c$

$$^3CT \cong C_0[(k_d + \gamma - k_c)/(k_d + 2\gamma - k_c)]\exp[-(k_1 + k(T))t] + C_0[\gamma/(k_d + 2\gamma - k_c)]\exp[-(k_d + \gamma)t] \quad (13)$$

$$\gamma = k_2k_{-2}/k_d$$

Since k_d is very large on the emission time scale, this reduces to eq 8.

Appendix II

An expression for the activation energies of **2** and **3** may be obtained from the known activation energies of **1** and **4** and the emission energies of all the complexes. Since the activation energies of **1** and **4** are known, the ratio gives a relation for E_1, E_4, and χ:

$$E_1 = 1.53E_4 + 0.53\chi \quad (14)$$

The energy differences for the mixed-ligand complexes, E_3 and E_2, may be expressed in terms of the emission energies, E_{em}, and the energy differences E_1 and E_4:

$$E_2 = \epsilon_2 + \tfrac{2}{3}E_1 + \tfrac{1}{3}E_4 \qquad E_3 = \epsilon_3 + \tfrac{1}{3}E_1 + \tfrac{2}{3}E_4$$

$$\epsilon_2 = \tfrac{2}{3}E_{em,1} + \tfrac{1}{3}E_{em,4} - E_{em,2} \quad (15)$$

$$\epsilon_3 = \tfrac{1}{3}E_{em,1} + \tfrac{2}{3}E_{em,4} - E_{em,3}$$

These are the same expressions as in the equilibrium case except that the correspondence of the energy difference between excited states and the activation energy is no longer justified. The mixed-complex activation energies may then be written in terms of the energy of **4** by employing eq 9, 14, and 15, which yields eq 10 (see text).

Registry No. $[Ru(dmb)_3](PF_6)_2$, 83605-44-1; $[Ru(dmb)_2(decb)](PF_6)_2$, 99617-91-1; $[Ru(dmb)(decb)_2](PF_6)_2$, 96897-29-9; $[Ru(decb)_3](PF_6)_2$, 75324-94-6; $[Ru(dmb)_3]^{3+}$, 47837-95-6; $[Ru(dmb)_2(decb)]^{3+}$, 99617-92-2; $[Ru(dmb)(decb)_2]^{3+}$, 96897-36-8; $[Ru(decb)_3]^{3+}$, 83605-72-5; $[Ru(dmb)_3]^{+}$, 65605-26-7; $[Ru(dmb)_2(decb)]^{+}$, 99617-93-3; $[Ru(dmb)(decb)_2]^{+}$, 96897-55-1; $[Ru(decb)_3]^{+}$, 83605-73-6; $Ru(dmb)_3$, 83605-52-1; $Ru(dmb)_2(decb)$, 99617-94-4; $Ru(dmb)(decb)_2$, 96897-62-0; $Ru(decb)_3$, 83605-74-7; $[Ru(dmb)_3]^{-}$, 83605-53-2; $[Ru(dmb)_2(decb)]^{-}$, 99617-95-5; $[Ru(dmb)(decb)_2]^{-}$, 96897-69-7; $[Ru(decb)_3]^{-}$, 83605-75-8; $Ru(dmb)_2Cl_2$, 68510-55-4; $Ru(decb)_2Cl_2$, 70281-20-8.

Contribution from the Chemistry Department, University of British Columbia, Vancouver, British Columbia, Canada V6T 1Y6

Trichloro-Bridged Diruthenium(II,III) Complexes: Preparation, Properties, and X-ray Structure of $Ru_2Cl_5(chiraphos)_2$ (chiraphos = 2(*S*),3(*S*)-Bis(diphenylphosphino)butane)

Ian S. Thorburn, Steven J. Rettig,[1] and Brian R. James*

Received June 7, 1985

The triply chloro-bridged, formally mixed-valence compounds $[RuCl(P\text{-}P)]_2(\mu\text{-}Cl)_3$ have been prepared by phosphine exchange from Ru(III) precursors containing PPh_3 or P(*p*-tolyl)$_3$ (P-P: chiraphos, 2(*S*),3(*S*)-bis(diphenylphosphino)butane; $PPh_2(CH_2)_nPPh_2$, n = 3 or 4; diop, 4(*S*),5(*S*)-bis((diphenylphosphino)methyl)-2,2-dimethyl-1,3-dioxolane). The chiraphos complex **1** has been characterized by X-ray analysis and is a highly symmetrical $(\mu\text{-}Cl)_3$ species with irregular octahedral geometry about each Ru (space group *P*1; a = 11.826 (2) Å, b = 11.968 (1) Å, c = 12.075 (2) Å, α = 112.333 (6)°, β = 92.409 (9)°, γ = 103.006 (7)°; Z = 1; the structure was refined to a conventional R value of 0.035 by using 6782 significant reflections and 405 variables). The crystallography data for **1**, and near-infrared spectral data in a range of solvents, show the dimers to be valence-delocalized. The complexes undergo disproportionation rapidly in CH_3CN and more slowly in Me_2SO and CH_3NO_2 to give dimeric Ru^{III}_2 and Ru^{II}_2 species. In CCl_4 or toluene, **1** exists in some other valence-delocalized form, possibly as a tetranuclear cluster.

Introduction

Previous work from this laboratory has described the use of $RuHCl(diop)_2$ as a catalyst for asymmetric hydrogenation (diop = 4(*S*),5(*S*)-bis((diphenylphosphino)methyl)-2,2-dimethyl-1,3-dioxolane).[2,3] Mechanistic studies revealed that the active species contained one diop per Ru(II) center, and this led us to investigate pathways to synthesize complexes containing Ru^{II}(P-P) moieties, where P-P is a chelating bis(tertiary phosphine) such as diop, chiraphos (2(*S*),3(*S*)-diphenylphosphino)butane), or a nonchiral analogue $PPh_2(CH_2)_nPPh_2$, where n = 4 (dppb), 3 (dppp), or 2 (dppe). Such catalysts would be analogous to the well-studied Rh^{I}(P-P) systems.[4-6] The complexes containing monodentate tertiary phosphines, $[RuCl_2(PR_3)_2]_2$, can be conveniently made by reduction of ruthenium(III) precursors such as $RuCl_3(PR_3)_2$,[7,8]

(1) Experimental Officer, University of British Columbia Crystal Structure Service.
(2) James, B. R.; McMillan, R. S.; Morris, R. H.; Wang, D. K. W. *Adv. Chem. Ser.* **1978**, *No. 167*, 122.
(3) James, B. R.; Wang, D. K. W. *Can. J. Chem.* **1980**, *58*, 245.
(4) Kagan, H. B. "Comprehensive Organometallic Chemistry"; Wilkinson, G., Ed.; Pergamon: Oxford, 1982; Vol. 8, p 463.
(5) Halpern, J. *Pure Appl. Chem.* **1983**, *55*, 99.
(6) Bakos, J.; Tóth, I.; Heil, B.; Markó, L. *J. Organomet. Chem.* **1985**, *279*, 23.
(7) James. B. R.; Thompson, L. K.; Wang, D. K. W. *Inorg. Chim. Acta* **1978**, *29*, L237.
(8) Dekleva, T. W.; Thorburn, I. S.; James, B. R. *Inorg. Chem. Acta* **1985**, *100*, 49.

0020-1669/86/1325-0234$01.50/0

Table I. Crystallographic Data[a]

compd	$(\mu\text{-Cl})_3[[(C_6H_5)_2PCH(CH_3)CH(CH_3)\text{-}P(C_6H_5)_2]RuCl]_2\cdot 2CH_2Cl_2$
formula	$C_{56}H_{56}Cl_5P_4Ru_2\cdot 2CH_2Cl_2$
fw	1402.22
cryst syst	triclinic
space group	$P\bar{1}$
a, Å	11.826 (2)
b, Å	11.968 (1)
c, Å	12.075 (2)
α, deg	112.333 (6)
β, deg	92.409 (9)
γ, deg	103.006 (7)
V, Å^3	1524.7 (4)
Z	1
D_c, g/cm^3	1.527
$F(000)$	709
μ(Mo Kα) cm^{-1}	10.24
cryst dimens, mm	0.11 × 0.43 × 0.45
transmissn factors	0.601–0.755
scan type	ω–2θ
scan range, deg in ω	0.60 + 0.35 tan θ
scan speed, deg/min	1.26–10.06
data collcd	$+h,\pm k,\pm l$
$2\theta_{max}$, deg	60
no. of unique reflcns	8838
no. of reflcns with $I \geq 3\sigma(I)$	6782
no. of variables	405
R	0.035
R_w	0.047
S	1.911
mean Δ/σ (final cycle)	0.05
max Δ/σ (final cycle)	0.82
residual density, e/Å^3	−0.92 to +0.75 (near Ru); $\sigma(\rho)$ = 0.03

[a] Conditions: temperature 22 °C; Enraf-Nonius CAD4-F diffractometer; Mo Kα radiation ($\lambda_{K\alpha_1}$ = 0.709 30, $\lambda_{K\alpha_2}$ = 0.713 59 Å); graphite monochromator; takeoff angle 2.7°; aperture (2.0 + tan θ) × 4.0 mm at a distance of 173 mm from the crystal; scan range extended by 25% on both sides for background measurement; $\sigma^2(I) = S + 2B + [0.04(S - B)]^2$ (S = scan count, B = normalized background count); function minimized $\sum w(|F_o| - |F_c|)^2$ where $w = 1/\sigma^2(F)$; $R = \sum||F_o| - |F_c||/\sum|F_o|$; $R_w = (\sum w(|F_o| - |F_c|)^2/\sum w|F_o|^2)^{1/2}$; $S = (\sum w(|F_o| - |F_c|)^2/(m - n))^{1/2}$. Values given for R, R_w, and S are based on those reflections with $I \geq 3\sigma(I)$.

and we thus attempted synthesis of $RuCl_3$(P-P) complexes from the same precursors via phosphine exchange.

The work led to the discovery of a new type of mixed-valence compounds, $[Ru_2Cl_2(P\text{-}P)_2](\mu\text{-}Cl)_3$, and this paper describes their synthesis, their characterization, and some solution chemistry.

Experimental Section

Physical Measurements. IR spectra were recorded on a Nicolet 5DX-FT-IR instrument as Nujol mulls between CsI plates. For near-IR spectra, a Cary 17D spectrophotometer and matched anaerobic quartz cells were employed; deuterated solvents were used when possible in order to minimize interference from solvent overtone bands. Visible spectra were recorded on a Perkin-Elmer 533A or Cary 17D spectrophotometer. Solution magnetic susceptibilities were measured by Evans' NMR method[9] using CH_2Cl_2 solutions containing ca. 2% *t*-BuOH at ambient temperatures while the Faraday method using an apparatus described elsewhere[10] was used for room-temperature, solid-state measurements. Solution electrical conductivities were measured at 25 °C under anaerobic conditions using a Thomas Serfass conductivity bridge and cell. Attempts to determine the molecular weights of the assumed dimer $[RuCl_3(dppb)]_2$ and the aggregated $[Ru_2Cl_5(chiraphos)_2]_n$ product were unsuccessful because of limited solubility. Microanalyses were performed by P. Borda of this department.

Materials and Methods. The preparation and solution studies of compounds were performed under an atmosphere of Ar or N_2 with dried and deoxygenated solvents. Phosphines (Strem Chemicals) were used as supplied for synthesis. The primary ruthenium source was $RuCl_3\cdot 3H_2O$

(9) Evans, D. F. *J. Chem. Soc.* **1959**, 2003.
(10) Herring, F. G.; Landa, B.; Thompson, R. C.; Schwerdtfeger, C. F. *J. Chem. Soc. A* **1971**, 528.

Table II. Final Positional and Isotropic Thermal Parameters with Estimated Standard Deviations in Parentheses[a]

atom	x	y	z	U_{eq}/U_{iso}[b]
Ru(1)	0	0	0	31
Ru(2)	3581 (5)	−14457 (5)	17345 (5)	32
Cl(1)	1919 (13)	5848 (12)	21163 (12)	37
Cl(2)	15588 (14)	−9983 (14)	2461 (13)	40
Cl(3)	−12774 (14)	−19360 (14)	1259 (14)	43
Cl(4)	−2024 (15)	−9485 (16)	−21394 (13)	49
Cl(5)	4732 (15)	−35399 (14)	9738 (15)	49
Cl(6)	1649 (36)	−51056 (29)	−33913 (34)	117
Cl(7)	24240 (42)	−34910 (68)	−24304 (68)	237
Cl(8)	−31794 (59)	−46900 (48)	−41029 (31)	172
Cl(9)	−32623 (66)	−50992 (61)	−19576 (50)	221
P(1)	−14574 (13)	8244 (14)	−3437 (13)	36
P(2)	12082 (13)	18138 (14)	1108 (13)	36
P(3)	−6818 (15)	−16908 (14)	32183 (14)	38
P(4)	19427 (15)	−10642 (15)	30898 (14)	40
C(1)	−856 (5)	1967 (6)	−989 (5)	42
C(2)	370 (6)	2757 (6)	−355 (6)	45
C(3)	278 (6)	−1870 (6)	4390 (5)	48
C(4)	1486 (6)	−2028 (6)	3959 (6)	49
C(5)	−1682 (7)	2795 (7)	−1021 (7)	58
C(6)	985 (8)	3439 (9)	−1088 (10)	77
C(7)	−274 (8)	−2937 (9)	4743 (8)	76
C(8)	2415 (8)	−1748 (8)	5029 (7)	65
C(9)	−2721 (6)	−293 (6)	−1448 (6)	46 (1)
C(10)	−2957 (7)	−326 (7)	−2599 (7)	58 (2)
C(11)	−3923 (7)	−1185 (8)	−3390 (8)	67 (2)
C(12)	−4648 (8)	−2004 (9)	−3055 (8)	72 (2)
C(13)	−4427 (8)	−2008 (9)	−1910 (8)	69 (2)
C(14)	−3451 (6)	−1156 (7)	−1129 (7)	54 (2)
C(15)	−2151 (5)	1688 (6)	925 (6)	44 (1)
C(16)	−1455 (6)	2489 (7)	2019 (6)	53 (1)
C(17)	−3121 (9)	3068 (9)	2875 (9)	77 (2)
C(18)	−1927 (8)	3204 (9)	2989 (8)	71 (2)
C(19)	−3824 (8)	2300 (8)	1794 (8)	68 (2)
C(20)	−3337 (6)	1597 (7)	818 (7)	54 (2)
C(21)	2495 (6)	1715 (6)	−696 (6)	44 (1)
C(22)	3376 (7)	2819 (7)	−461 (7)	61 (2)
C(23)	4374 (8)	2689 (9)	−1039 (9)	73 (2)
C(24)	4545 (8)	1596 (9)	−1695 (9)	74 (2)
C(25)	3694 (8)	493 (9)	−1913 (8)	70 (2)
C(26)	2680 (6)	575 (6)	−1424 (6)	51 (1)
C(27)	1983 (5)	2868 (6)	1637 (5)	43 (1)
C(28)	2822 (6)	2453 (7)	2115 (6)	52 (1)
C(29)	3444 (7)	3167 (7)	3262 (7)	57 (2)
C(30)	3228 (9)	4285 (9)	3948 (9)	74 (2)
C(31)	2427 (9)	4707 (10)	3496 (9)	79 (2)
C(32)	1781 (7)	4005 (8)	2330 (7)	62 (2)
C(33)	−2014 (6)	−2940 (7)	2790 (6)	50 (2)
C(34)	−2289 (6)	−3925 (7)	1654 (6)	52 (1)
C(35)	−3320 (7)	−4883 (8)	1375 (8)	64 (2)
C(36)	−4087 (7)	−4831 (7)	2222 (7)	60 (2)
C(37)	−3847 (8)	−3871 (8)	3326 (8)	67 (2)
C(38)	−2817 (7)	−2926 (7)	3626 (7)	59 (2)
C(39)	−1285 (5)	−368 (6)	4039 (6)	44 (1)
C(40)	−879 (6)	500 (7)	5194 (6)	50 (1)
C(41)	−1376 (7)	1516 (8)	5706 (8)	65 (2)
C(42)	−2293 (8)	1618 (9)	5059 (9)	72 (2)
C(43)	−2715 (8)	755 (8)	3885 (8)	69 (2)
C(44)	−2205 (7)	−236 (7)	3362 (7)	61 (2)
C(45)	3167 (5)	−1561 (6)	2367 (6)	44 (1)
C(46)	3923 (7)	−789 (7)	1960 (7)	59 (2)
C(47)	4832 (8)	−1145 (9)	1348 (8)	72 (2)
C(48)	4980 (10)	−2330 (10)	1115 (10)	83 (3)
C(49)	4195 (9)	−3144 (10)	1464 (9)	79 (2)
C(50)	3306 (7)	−2757 (7)	2109 (7)	61 (2)
C(51)	2612 (6)	513 (6)	4236 (6)	46 (1)
C(52)	3792 (7)	884 (7)	4740 (7)	59 (2)
C(53)	4252 (8)	2035 (9)	5683 (9)	73 (2)
C(54)	3551 (8)	2830 (9)	6129 (9)	71 (2)
C(55)	2386 (7)	2473 (7)	5653 (7)	61 (2)
C(56)	1925 (6)	1331 (7)	4697 (6)	52 (1)
C(57)	1003 (10)	−3716 (11)	−2218 (11)	94 (3)
C(58)	−2620 (10)	−4144 (11)	−2612 (10)	90 (3)

[a] Fractional coordinates are ×10^5 except for C atoms (×10^4); U values are ×10^3 Å^2. [b] $U_{eq} = {}^1/_3$ trace (diagonalized U).

Table III. Bond Lengths (Å) with Estimated Standard Deviations in Parentheses

Ru(1)–Cl(1)	2.3648 (13)	C(15)–C(20)	1.379 (10)
Ru(1)–Cl(2)	2.4756 (15)	C(16)–C(17)	2.382 (12)
Ru(1)–Cl(3)	2.5268 (15)	C(17)–C(18)	1.380 (14)
Ru(1)–Cl(4)	2.3700 (14)	C(18)–C(19)	2.395 (13)
Ru(1)–P(1)	2.2655 (15)	C(19)–C(20)	1.396 (11)
Ru(1)–P(2)	2.2668 (15)	C(21)–C(22)	1.407 (10)
Ru(2)–Cl(1)	2.3511 (13)	C(21)–C(26)	1.386 (9)
Ru(2)–Cl(2)	2.4773 (15)	C(22)–C(23)	1.405 (12)
Ru(2)–Cl(3)	2.4830 (15)	C(23)–C(24)	1.314 (13)
Ru(2)–Cl(5)	2.3575 (14)	C(24)–C(25)	1.393 (13)
Ru(2)–P(3)	2.2871 (15)	C(25)–C(26)	1.365 (12)
Ru(2)–P(4)	2.2776 (15)	C(27)–C(28)	1.399 (9)
Cl(6)–C(57)	1.762 (13)	C(27)–C(32)	1.381 (10)
Cl(7)–C(57)	1.687 (13)	C(28)–C(29)	1.386 (10)
Cl(8)–C(58)	1.708 (12)	C(29)–C(30)	1.368 (12)
Cl(9)–C(58)	1.690 (12)	C(30)–C(31)	1.353 (14)
P(1)–C(1)	1.844 (6)	C(31)–C(32)	1.412 (13)
P(1)–C(9)	1.838 (7)	C(33)–C(34)	1.392 (10)
P(1)–C(15)	1.836 (6)	C(33)–C(38)	1.412 (11)
P(2)–C(2)	1.874 (6)	C(34)–C(35)	1.398 (11)
P(2)–C(21)	1.843 (6)	C(35)–C(36)	1.389 (12)
P(2)–C(27)	1.843 (6)	C(36)–C(37)	1.354 (12)
P(3)–C(3)	1.881 (6)	C(37)–C(38)	1.388 (12)
P(3)–C(33)	1.808 (7)	C(39)–C(40)	1.368 (9)
P(3)–C(39)	1.836 (6)	C(39)–C(44)	1.408 (10)
P(4)–C(4)	1.847 (6)	C(40)–C(41)	1.410 (11)
P(4)–C(45)	1.820 (6)	C(41)–C(42)	1.365 (13)
P(4)–C(51)	1.832 (7)	C(42)–C(43)	1.386 (13)
C(1)–C(2)	1.524 (9)	C(43)–C(44)	1.397 (12)
C(1)–C(5)	1.548 (9)	C(45)–C(46)	1.380 (10)
C(2)–C(6)	1.521 (10)	C(45)–C(50)	1.394 (10)
C(3)–C(4)	1.567 (10)	C(46)–C(47)	1.385 (12)
C(3)–C(7)	1.517 (10)	C(47)–C(48)	1.391 (14)
C(4)–C(8)	1.542 (9)	C(48)–C(49)	1.389 (15)
C(9)–C(10)	1.390 (10)	C(49)–C(50)	1.393 (13)
C(9)–(14)	1.375 (10)	C(51)–C(52)	1.401 (10)
C(10)–C(11)	1.382 (12)	C(51)–C(56)	1.381 (10)
C(11)–C(12)	1.346 (13)	C(52)–C(53)	1.381 (13)
C(12)–C(13)	1.397 (13)	C(53)–C(54)	1.373 (13)
C(13)–C(14)	1.381 (12)	C(54)–C(55)	1.376 (12)
C(15)–C(16)	1.390 (10)	C(55)–C(56)	1.383 (11)

Table IV. Bond Angles (deg) with Estimated Standard Deviations in Parentheses

Cl(1)–Ru(1)–Cl(2)	80.24 (5)	C(3)–C(4)–C(8)	111.3 (6)
Cl(1)–Ru(1)–Cl(3)	78.90 (5)	P(1)–C(9)–C(10)	123.2 (5)
Cl(1)–Ru(1)–Cl(4)	169.76 (5)	P(1)–C(9)–C(14)	118.4 (5)
Cl(1)–Ru(1)–P(1)	102.93 (5)	C(10)–C(9)–C(14)	118.5 (6)
Cl(1)–Ru(1)–P(2)	94.80 (5)	C(9)–C(10)–C(11)	120.6 (7)
Cl(2)–Ru(1)–Cl(3)	81.53 (5)	C(10)–C(11)–C(12)	120.3 (8)
Cl(2)–Ru(1)–Cl(4)	92.81 (5)	C(11)–C(12)–C(13)	120.6 (9)
Cl(2)–Ru(1)–P(1)	176.48 (6)	C(12)–C(13)–C(14)	118.8 (8)
Cl(2)–Ru(1)–P(2)	96.64 (5)	C(9)–C(14)–C(13)	121.2 (7)
Cl(3)–Ru(1)–Cl(4)	92.71 (6)	P(1)–C(15)–C(16)	119.1 (5)
Cl(3)–Ru(1)–P(1)	97.49 (5)	P(1)–C(15)–C(20)	122.1 (5)
Cl(3)–Ru(1)–P(2)	173.64 (5)	C(16)–C(15)–C(20)	118.8 (6)
Cl(4)–Ru(1)–P(1)	83.84 (5)	C(15)–C(16)–C(17)	90.9 (5)
Cl(4)–Ru(1)–P(2)	93.46 (6)	C(16)–C(17)–C(18)	30.7 (5)
P(1)–Ru(1)–P(2)	84.69 (5)	C(17)–C(18)–C(19)	29.6 (5)
Cl(1)–Ru(2)–Cl(2)	80.47 (5)	C(18)–C(19)–C(20)	90.2 (6)
Cl(1)–Ru(2)–Cl(3)	80.05 (5)	C(15)–C(20)–C(19)	120.3 (7)
Cl(1)–Ru(2)–Cl(5)	169.44 (5)	P(2)–C(21)–C(22)	118.9 (5)
Cl(1)–Ru(2)–P(3)	95.87 (5)	P(2)–C(21)–C(26)	121.8 (5)
Cl(1)–Ru(2)–P(4)	102.10 (5)	C(22)–C(21)–C(26)	119.0 (6)
Cl(2)–Ru(2)–Cl(3)	82.38 (5)	C(21)–C(22)–C(23)	116.9 (7)
Cl(2)–Ru(2)–Cl(5)	91.70 (5)	C(22)–C(23)–C(24)	122.8 (9)
Cl(2)–Ru(2)–P(3)	175.24 (6)	C(23)–C(24)–C(25)	120.8 (9)
Cl(2)–Ru(2)–P(4)	93.91 (6)	C(24)–C(25)–C(26)	118.4 (8)
Cl(3)–Ru(2)–Cl(5)	91.95 (5)	C(21)–C(26)–C(25)	121.9 (7)
Cl(3)–Ru(2)–P(3)	100.05 (6)	P(2)–C(27)–C(28)	116.2 (5)
Cl(3)–Ru(2)–P(4)	175.39 (6)	P(2)–C(27)–C(32)	125.0 (5)
Cl(5)–Ru(2)–P(3)	92.30 (6)	C(28)–C(27)–C(32)	118.8 (6)
Cl(5)–Ru(2)–P(4)	85.39 (6)	C(27)–C(28)–C(29)	120.9 (6)
P(3)–Ru(2)–P(4)	83.85 (6)	C(28)–C(29)–C(30)	119.9 (7)
Ru(1)–Cl(1)–Ru(2)	87.16 (4)	C(29)–C(30)–C(31)	120.0 (9)
Ru(1)–Cl(2)–Ru(2)	82.05 (5)	C(30)–C(31)–C(32)	121.5 (9)
Ru(1)–Cl(3)–Ru(2)	80.92 (4)	C(27)–C(32)–C(31)	118.9 (7)
Ru(1)–P(1)–C(1)	107.9 (2)	P(3)–C(33)–C(34)	122.4 (5)
Ru(1)–P(1)–C(9)	115.4 (2)	P(3)–C(33)–C(38)	119.5 (6)
Ru(1)–P(1)–C(15)	119.8 (2)	C(34)–C(33)–C(38)	118.1 (7)
C(1)–P(1)–C(9)	105.2 (3)	C(33)–C(34)–C(35)	120.2 (7)
C(1)–P(1)–C(15)	104.3 (3)	C(34)–C(35)–C(36)	119.8 (8)
C(9)–P(1)–C(15)	102.8 (3)	C(35)–C(36)–C(37)	121.0 (8)
Ru(1)–P(2)–C(2)	111.1 (2)	C(36)–C(37)–C(38)	119.9 (8)
Ru(1)–P(2)–C(21)	117.7 (2)	C(33)–C(38)–C(37)	121.0 (7)
Ru(1)–P(2)–C(27)	114.6 (2)	P(3)–C(39)–C(40)	125.9 (5)
C(2)–P(2)–C(21)	108.9 (3)	P(3)–C(39)–C(44)	114.8 (5)
C(2)–P(2)–C(27)	105.0 (3)	C(40)–C(39)–C(44)	119.3 (6)
C(21)–P(2)–C(27)	98.3 (3)	C(39)–C(40)–C(41)	120.6 (6)
Ru(2)–P(3)–C(3)	110.5 (2)	C(40)–C(41)–C(42)	119.8 (8)
Ru(2)–P(3)–C(33)	118.7 (2)	C(41)–C(42)–C(43)	120.6 (8)
Ru(2)–P(3)–C(39)	114.1 (2)	C(42)–C(43)–C(44)	119.8 (8)
C(3)–P(3)–C(33)	107.3 (3)	C(39)–C(44)–C(43)	119.8 (7)
C(3)–P(3)–C(39)	106.1 (3)	P(4)–C(45)–C(46)	119.8 (5)
C(33)–P(3)–C(39)	98.8 (3)	P(4)–C(45)–C(50)	121.6 (5)
Ru(2)–P(4)–C(4)	106.7 (2)	C(46)–C(45)–C(50)	118.3 (6)
Ru(2)–P(4)–C(45)	112.8 (2)	C(45)–C(46)–C(47)	122.4 (7)
Ru(2)–P(4)–C(51)	121.1 (2)	C(46)–C(47)–C(48)	119.0 (9)
C(4)–P(4)–C(45)	106.2 (3)	C(47)–C(48)–C(49)	119.5 (9)
C(4)–P(4)–C(51)	104.8 (3)	C(48)–C(49)–C(50)	120.5 (9)
C(45)–P(4)–C(51)	104.1 (3)	C(45)–C(50)–C(49)	120.1 (8)
P(1)–C(1)–C(2)	111.6 (4)	P(4)–C(51)–C(52)	121.5 (5)
P(1)–C(1)–C(5)	113.0 (5)	P(4)–C(51)–C(56)	119.9 (5)
C(2)–C(1)–C(5)	111.5 (5)	C(52)–C(51)–C(56)	118.3 (6)
P(2)–C(2)–C(1)	110.9 (4)	C(51)–C(52)–C(53)	120.6 (7)
P(2)–C(2)–C(6)	115.6 (5)	C(52)–C(53)–C(54)	120.0 (9)
C(1)–C(2)–C(6)	111.2 (6)	C(53)–C(54)–C(55)	120.1 (9)
P(3)–C(3)–C(4)	110.7 (4)	C(54)–C(55)–C(56)	120.1 (7)
P(3)–C(3)–C(7)	114.2 (5)	C(51)–C(56)–C(55)	120.8 (7)
C(4)–C(3)–C(7)	109.5 (6)	Cl(6)–C(57)–Cl(7)	109.4 (7)
P(4)–C(4)–C(3)	109.8 (4)	Cl(8)–C(58)–Cl(9)	111.9 (7)
P(4)–C(4)–C(8)	113.1 (5)		

(42.3% Ru) obtained from Johnson Matthey Ltd. The precursor compounds $RuCl_3(PR_3)_2(DMA)\cdot DMA$, R = Ph[11] or *p*-tolyl,[12] were prepared by the literature procedure but with DMA (*N,N*-dimethylacetamide) as solvent rather than the reported methanol.[13]

Preparation of Compounds. Tris(μ-chloro)dichlorobis(bidentate phosphine)diruthenium(II,III), $Ru_2Cl_5(P\text{-}P)_2$. P-P = 1,4-Bis(diphenylphosphino)butane (dppb) and diop. A suspension of $RuCl_3(PPh_3)_2(DMA)\cdot DMA$ (1 g, 1.1 mmol) and the bidentate phosphine (mole ratio 1:1) was refluxed in 150 mL of hexanes under N_2 for 24 h. The red-brown product was filtered, washed well with hexanes, and vacuum-dried. Recrystallization form CH_2Cl_2–ether gave air-stable, red powders. $Ru_2Cl_5(dppb)_2$: Yield 0.49 g (72%). Anal. Calcd for $C_{56}H_{56}Cl_5P_4Ru_2$: C, 54.57; H, 4.59; Cl, 14.38. Found: C, 54.7; H, 4.6; Cl, 14.2. $Ru_2Cl_5(diop)_2$: Yield 0.50 g (66%). Anal. Calcd for $C_{62}H_{64}O_4Cl_5P_4Ru_2$: C, 54.09; H, 4.65; Cl, 12.90. Found: C, 53.9; H, 4.8; Cl, 12.8.

P-P = chiraphos or 1,3-Bis(diphenylphosphino)propane (dppp). The preparative procedure for these complexes is the same as that above, but with $RuCl_3(p\text{-tolyl})_3)_2(DMA)\cdot DMA$ (1.0 g, 1.0 mmol) as precursor. Dichloromethane solvate could be readily removed on pumping. $Ru_2Cl_5(chiraphos)_2$ (**1**): Yield 0.51 g (82%). Anal. Calcd for $C_{56}H_{56}Cl_5P_4Ru_2$: C, 54.57; H, 4.59; Cl, 14.38. Found: C, 54.7; H, 4.6; Cl, 14.2. $Ru_2Cl_5(dppp)_2$: Yield 0.26 g (43%). Anal. Calcd for $C_{54}H_{52}Cl_5P_4Ru_2$: C, 53.84; H, 4.32; Cl, 14.75. Found: C, 53.7; H, 4.5; Cl, 14.6. Crystals of **1** containing two molecules of CH_2Cl_2 solvate were found suitable for X-ray analysis.

Trichloro(1,4-bis(diphenylphosphino)butane)ruthenium(III) Dimer. $[RuCl_3(dppb)]_2$ (2). To $RuCl_5(dppb)_2$ (1.0 g, 0.81 mmol) in CH_3CN (60 mL) was added $AgPF_6$ (0.103 g, 0.41 mmol) in CH_3CN (10 mL), and the mixture was stirred for 0.5 h. AgCl was filtered from the pink solution by using Celite and the filtrate evaporated to a red oil. Addition of benzene (50 mL) and rapid stirring for 16 h caused precipitation of a solid that was filtered and washed with benzene (30 mL). The filtrate and washings were combined and concentrated to 10 mL and hexanes (40 mL) added to cause precipitation of a red-brown solid. This was filtered out, washed well with hexanes, and vacuum-dried. The product

(11) Wang, D. K. W. Ph.D. Dissertation, University of British Columbia, 1978.
(12) Thorburn, I. S. M.Sc. Dissertation, University of British Columbia, 1980.
(13) Stephenson, T. A.; Wilkinson, G. *J. Inorg. Nucl. Chem.* **1966**, *28*, 945.

Table V. Intraannular Torsion Angles (deg) with Standard Deviations in Parentheses

P(2)–Ru(1)–P(1)–C(1)	25.0 (2)
Ru(1)–P(1)–C(1)–C(2)	−41.5 (5)
P(1)–C(1)–C(2)–P(2)	34.7 (5)
Ru(1)–P(2)–C(2)–C(1)	−14.0 (5)
P(1)–Ru(1)–P(2)–C(2)	−8.4 (2)
P(4)–Ru(2)–P(3)–C(3)	−15.0 (2)
Ru(2)–P(3)–C(3)–C(4)	−9.3 (5)
P(3)–C(3)–C(4)–P(4)	35.5 (5)
Ru(2)–P(4)–C(4)–C(3)	−47.6 (5)
P(3)–Ru(2)–P(4)–C(4)	32.4 (2)

was recrystallized from CH_2Cl_2–hexanes to give an air-stable maroon compound, yield 0.18 g (35%). Anal. Calcd for $C_{56}H_{56}Cl_6P_4Ru_2$; C, 53.00; H, 4.42; Cl, 16.8. Found: C, 52.9; H, 4.5; Cl, 16.6. IR: ν(Ru–Cl) 352 cm^{-1}. μ_{eff}: 1.98 μ_B/Ru. The yellow Ru(II) dimer $[Ru_2Cl_3(dppb)_2(CH_3CN)_2]^+PF_6^-$ (**3**) has been isolated from the benzene-insoluble material.[14]

Crystallographic Study of $Ru_2Cl_5(chiraphos)_2$ (1). Crystallographic data appear in Table I. The crystal was mounted in a general orientation, lattice constants being determined by least squares on (2 sin θ)/λ values for 25 reflections (with 2θ = 40–46°), measured with Mo $K\alpha_1$ radiation. The intensities of three standard reflections (monitored each hour of X-ray exposure time) showed only small random fluctuations during the data collection. The data were processed[15] and corrected for absorption by using the Gaussian integration method[16,17] (96 sampling points).

The noncentrosymmetric space group $P1$ is determined by the chirality of the phosphine ligands. The structure was solved by conventional heavy-atom methods, the coordinates of the Ru, Cl, and P atoms being determined from the Patterson function and those of the remaining non-hydrogen atoms from a subsequent difference map. The coordinates of Ru(1) were fixed to determine the origin. The phenyl and solvent carbon atoms were refined with isotropic thermal parameters, and all other non-hydrogen atoms with anisotropic thermal parameters were calculated (methyl groups staggered; $C(sp^3)$–H = 0.98 Å, $C(sp^2)$–H = 0.97 Å) and included as fixed contributors in subsequent cycles of refinement. Although there are sufficient data to refine all non-hydrogen atoms with anisotropic thermal parameters, the additional structural information to be gained was judged to relatively minor in comparison with the cost of the additional computations.

Neutral-atom scattering factors for all atoms and anomalous scattering factors for Ru, Cl, and P atoms were taken from ref 18.

The absolute configuration has been confirmed by parallel refinement, the R and R_w ratios being 1.0126 and 1.0134, respectively. Final positional and equivalent isotropic thermal parameters are given in Table II. Bond lengths, bond angles, and intraannular torsion angles appear in Tables III–V, respectively. Calculated coordinates and temperature factors for H atoms, anisotropic thermal parameters, a complete listing of torsion angles, and observed and calculated structure factor amplitudes (Tables VI–IX) are included as supplementary material.

Results

Synthesis. Refluxing $RuCl_3(PR_3)_2(DMA)\cdot DMA$ with 1 equiv of bis(tertiary phosphine), P-P, in hexanes under anaerobic conditions led to the exchange of the PR_3 ligands by the bidentate phosphine. The exchange was unexpectedly accompanied by reduction and dimerization to produce in high yield the insoluble, mixed-valence complexes $Ru_2Cl_5(P\text{-}P)_2$, containing three bridging chloride ligands. The exchange was confirmed in all cases by the ^1H NMR spectra of the free monodentate phosphine, isolated from the filtrate after removal of the insoluble red product. The $^{31}P\{^1H\}$ NMR showed some free phosphine oxide in the 1:6 OPR_3:PR_3 ratio, which is close to that expected (1:7) for the reduction of 50% of the Ru(III) by the phosphine (eq 1). Trace water in the

$$4RuCl_3(PR_3)_2 + 4P\text{-}P \xrightarrow{H_2O} 2Ru_2Cl_5(P\text{-}P)_2 + OPR_3 + 7PR_3 + 2HCl \quad (1)$$

presence of the phosphine is considered to be the only possible reagent responsible for the redox process.

The solution μ_{eff} values for the mixed-valence compounds were 1.95 and 1.78 μ_B for the chiraphos and diop systems, respectively, the values being consistent with one unpaired electron per molecule. The paramagnetic shifts for the dppp and dppb complexes, because of limited solubility, could not be measured accurately. However, a Faraday measurement on the $Ru_2Cl_5(dppb)_2$ complex yielded μ_{eff} = 1.92 μ_B.

The IR spectra of the $Ru_2Cl_5(P\text{-}P)_2$ complexes all show a band at 340 ± 5 cm^{-1}, characteristic of terminal Ru–Cl stretching.

Attempts to prepare the 1,2-bis(diphenylphosphino)ethane analogue, $Ru_2Cl_5(dppe)_2$, via phosphine exchange have been unsuccessful to date, with *trans*-$RuCl_2(dppe)_2$[19] being the only product isolated in significant yield. Both dppe and chiraphos form five-membered ring systems, so the reason for the difference in reactivity is not obvious; it may be simply a question of relative solubilities.

In addition to the isolated $Ru_2Cl_5(P\text{-}P)_2$ complexes, small amounts (<10% of the total yield) of Ru(II) species were obtained by workup of the filtrate following recrystallization. Yellow crystals of *trans*-$RuCl_2(chiraphos)_2$[20] and green crystals of $[RuCl_2(dppb)_{1.5}]_2$[2,21] were isolated and characterized.

X-ray Crystal Structure of Tris(μ-chloro)dichlorobis(chiraphos)diruthenium(II,III). The $Ru_2Cl_5(P\text{-}P)_2$ complexes after recrystallization were usually obtained as red powders; the exception was the chiraphos derivative, which invariably formed dark red crystals. A single X-ray diffraction study showed the complex to be a μ_3-chloro-bridged complex (Figure 1), with a near-twofold axis through the bridging chloride Cl(1). The coordination geometry about each ruthenium is irregular octahedral, and the metal to ligand bond distances and angles are essentially identical (Tables III and IV, respectively). The bridging chloride Cl(1) trans to terminal chlorides has shorter Ru–Cl distances (average 2.364 (1) Å), compared to those of the bridging chloro ligands trans to phosphorus (average 2.491 (2) Å). This clearly results from the weaker trans influence of the chloro ligands and produces a wider Ru–Cl(1)–Ru bond angle compared to the other two Ru–Cl–Ru angles. Two regular octahedra sharing one face have a bridging angle θ of 70.5° (given by cos (θ/2) = (2/3).[22] In the chiraphos complex the average bridging angle is 83.4°, and hence the ruthenium atoms are further apart than expected for a regular cofacial bioctahedron. The distance between the ruthenium centers (3.25 Å) is well outside the range (2.28–2.95 Å) usually found for a Ru–Ru bond.[8,23–25] The Ru–P and Ru–Cl bond lengths are comparable to those found in both dimeric Ru(II)[26] and dimeric Ru(III)[8] complexes containing tertiary phosphines. Chioccala and Daly[22] have elucidated the structure of $Ru_2Cl_5(P\text{-}n\text{-}Bu_3)_4$, which is similar but is unsymmetrical in that one of the octahedra has been rotated by ±120° about the Ru–Ru vector. As with the chiraphos complex, the crystallographic data do not permit assignment of formal valence states to the ruthenium atoms.

Electronic Absorption Spectra. Intervalence charge-transfer transitions are a characteristic feature of mixed-valence complexes, and those of Ru(II)–Ru(III) systems have been widely studied.[27,28]

(14) Thorburn, I. S.; Rettig, S. J.; James, B. R. *J. Organomet. Chem.* **1985**, *296*, 103.
(15) The computer programs used include locally written programs for data processing and locally modified versions of the following: ORFLS (full-matrix least squares) and ORFFE (function and errors) by W. R. Busing, K. O. Martin, and H. A. Levy; FORDAP (Patterson and Fourier syntheses) by A. Zalkin; ORTEP II (illustrations) by C. K. Johnson.
(16) Coppens, P.; Leiserowitz, L.; Rabinovich, D. *Acta Crystallogr.* **1965**, *18*, 1035.
(17) Busing, W. R.; Levy, H. A. *Acta Crystallogr.* **1967**, *22*, 457.
(18) "International Tables for X-ray Crystallography"; Kynoch Press: Birmingham, England, 1974; Vol. IV.
(19) Mason, R.; Meek, D. W.; Scollary, G. R. *Inorg. Chim. Acta* **1976**, *16*, L11.
(20) Thorburn, I. S.; Rettig, S. J.; James, B. R., to be submitted for publication.
(21) Bressan, M.; Rigo, P. *Inorg. Chem.* **1975**, *14*, 2286.
(22) Chioccola, G.; Daly, J. J. *J. Chem. Soc. A* **1968**, 1981.
(23) Mattson, B. M.; Heiman, J. R.; Pignolet, L. H. *Inorg. Chem.* **1976**, *15*, 564 and references therein.
(24) Schummann, H.; Opitz, J.; Pickardt, J. *J. Organomet. Chem.* **1977**, *128*, 253.
(25) Jones, R. A.; Wilkinson, G.; Coloquohoun, I. J.; McFarlane, W.; Galas, A. M. R.; Hurthouse, M. B. *J. Chem. Soc., Dalton Trans.* **1980**, 2480.
(26) Fraser, A. J. F.; Gould, R. O. *J. Chem. Soc., Dalton Trans.* **1974**, 1139.

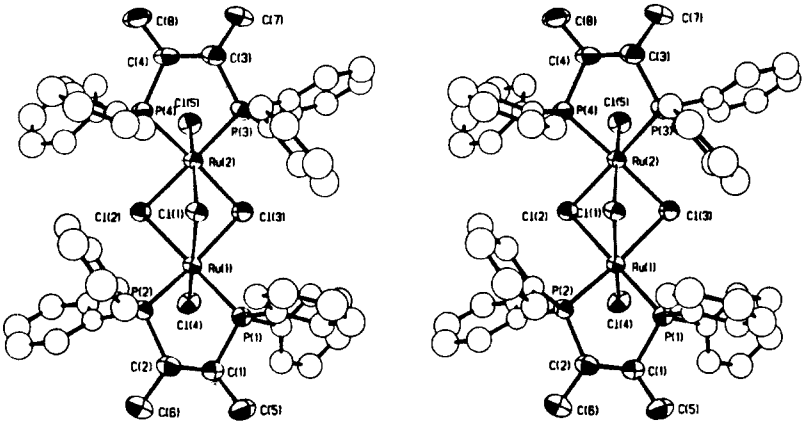

Figure 1. Stereoview of the $[RuCl(chiraphos]_2(\mu\text{-}Cl)_3$ molecule. Thermal ellipsoids shown have 50% probability, hydrogen atoms being omitted for the sake of clarity.

The synthesized $Ru_2Cl_5(P\text{-}P)_2$ complexes in solution exhibit absorptions in the near-IR that are absent in the Ru^{II}_2 and Ru^{III}_2 congeners (see below) and are therefore assigned to such transitions.

The $Ru_2Cl_5(chiraphos)_2$ complex (**1**) was most extensively studied, and the data for the near-IR bands observed are summarized in Table X. In $CDCl_3$, **1** obeys Beer's law; however, the presence of a principal absorption at 2350 nm and a second less intense one at 1090 nm (Figure 2) suggests the presence of more than one species. Unfortunately, the absorption spectrum at longer wavelengths (>2600 nm) could not be studied because of the limitations of the spectrometer, and consequently the values of $\Delta\nu_{1/2}$ were estimated by assuming a Gaussian band shape and doubling the bandwidth at half-height on just the high-energy side of the band. The calculated $\Delta\nu_{1/2}$ values for a class II system (see Discussion) were determined from $\nu_{max} = (\Delta\nu_{1/2})^2/2310$ cm^{-1}, where ν_{max} is the energy of the intervalence transition (IT) at 300 K. With the exception of CCl_4 and toluene, the position of the lower energy band is essentially solvent-independent. Further, the solid-state spectrum (KBr) of **1** shows the same low-energy absorption (2350 nm) as that found in most solutions. The higher energy transition does show more solvent dependency; however, the unsymmetrical band shape (inset, Figure 2) suggests this absorption is composite in character.

In CCl_4 or toluene the near-IR spectrum of **1** is very different from that in $CDCl_3$ (Figure 2). The principal absorption is now seen at 880 nm, and only very broad absorption is found at lower energy. Evaporation of a CCl_4 solution produces solid **1a**, whose

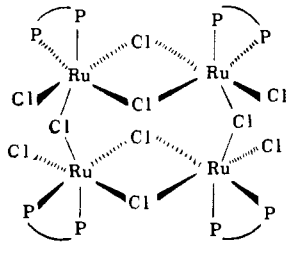

1a

solid-state spectrum is identical with that observed in solution; nevertheless, redissolving **1a** in $CDCl_3$ yields the same near-IR spectrum found with **1** in this solvent. The major differences observed in the near-IR spectra for CCl_4 and $CDCl_3$ solutions of **1** are accompanied also by changes in the visible region (Figure 3).

The $Ru_2Cl_5(chiraphos)_2$ complex did not give stable spectra in all solvents tried. In $Me_2SO\text{-}d_6$ and CD_3NO_2, the intensity of the near-IR bands decreased to zero after 1 and 5 h, respectively. In CD_3CN, no near-IR bands were detected, implying an instantaneous loss of absorption upon dissolution. The visible spectra of the $Me_2SO\text{-}d_6$ and CD_3NO_2 solutions after loss of the near-IR absorption were the same but were markedly different from that measured in CH_3CN (Figure 3).

As well as being solvent-dependent, the near-IR absorptions for the $Ru_2Cl_5(P\text{-}P)_2$ complexes are also dependent on the bis(tertiary phosphine) (Figure 4, Table X). The more limited data for $Ru_2Cl_5(dppb)_2$ indicate that the positions of both absorptions do not vary with solvent, including CCl_4, although in CH_3CN or $Me_2SO\text{-}d_6$ the dppb complex undergoes changes analogous to those observed for the chiraphos complex. The visible spectra of the dppp, dppb, and diop complexes in $CDCl_3$ are all similar to that found for **1** in this solvent (Figure 3) and exhibit principal absorption maxima in the range 360–400 nm ($\epsilon \sim 4000$ M^{-1} cm^{-1}).

Table X. Near-Infrared Spectral Data at Room Temperature for $Ru_2Cl_5(P\text{-}P)$ Complexes

solvent	λ_{max}, nm (ν, cm^{-1})	ϵ, M^{-1} cm^{-1}	$\Delta\nu_{1/2}$,[a] cm^{-1} found	$\Delta\nu_{1/2}$,[a] cm^{-1} calcd
	P-P = chiraphos			
CD_3NO_2	2340 (4270)	5530[b]	1660	3140
	1150 (8700)	490[b]	5030	4480
$C_4H_6O_3$[c]	2340 (4270)	5510	1650	3140
	1150 (8700)	530	3600	4480
DMA	2340 (4270)	5460[b]	1650	3140
	1120 (8930)	510[b]	5380	4540
$Me_2SO\text{-}d_6$	2350 (4260)	*d*	*d*	*d*
	1190 (8400)	*d*	*d*	*d*
$CDCl_3$	2350 (4260)	5540	1630	3140
	1090 (9170)	660	4410	4600
$C_6H_5CH_3$	~2050 (4880)[e]	1100	*e*	*e*
	880 (11360)	2060	3580	5120
CCl_4	~2050 (4880)[e]	1030	*e*	*e*
	880 (11360)	2170	3320	5120
	P-P = dppb			
DMA	~2050 (4880)	850	*e*	*e*
	970 (10310)	540	3040	4880
$CDCl_3$	~2050 (4880)	1180	*e*	*e*
	970 (10310)	890	3040	4880
CCl_4	~2050 (4880)	1290	*e*	*e*
	970 (10310)	1080	3100	4880
	P-P = diop			
DMA	~2050 (4880)	1140	*e*	*e*
	950 (10530)	784	2940	4932
$CDCl_3$	~2050 (4880)	1410	*e*	*e*
	950 (10530)	1030	2940	4932
	P-P = dppp			
$CDCl_3$	2060 (4850)	2070	3500	3350
	960 (10420)	1590	3650	4910

[a] Bandwidth at half-height (see text). [b] ϵ values calculated from initial absorbance. [c] Propylene carbonate. [d] Initial absorbance decays rapidly. [e] Absorption is too broad to estimate values of $\Delta\nu_{1/2}$.

(27) Creutz, C. *Prog. Inorg. Chem.* **1983**, *30*, 1.
(28) Meyer, T. J. *Acc. Chem. Res.* **1978**, *11*, 94.

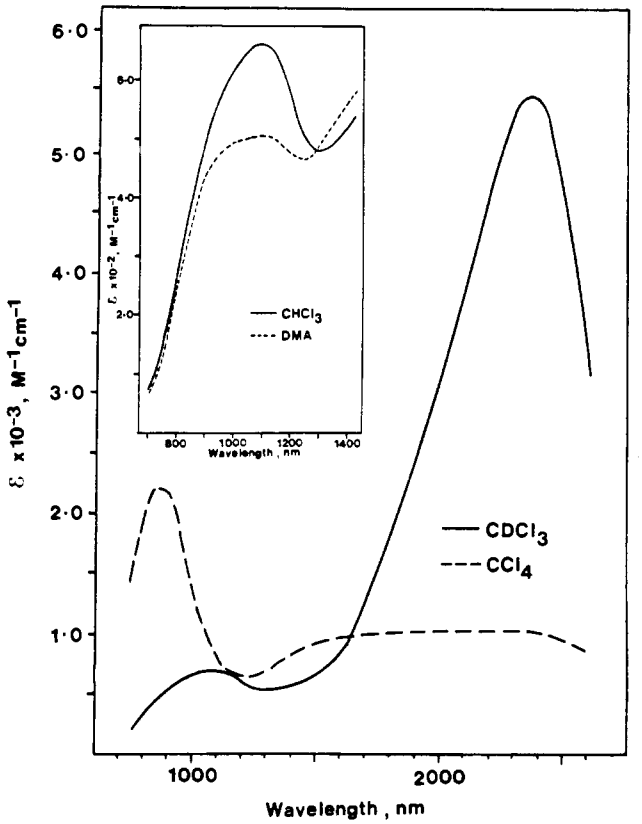

Figure 2. Near-IR spectra of $Ru_2Cl_5(chiraphos)_2$ in $CDCl_3$ and CCl_4. Inset shows the higher energy absorption in $CHCl_3$ and DMA.

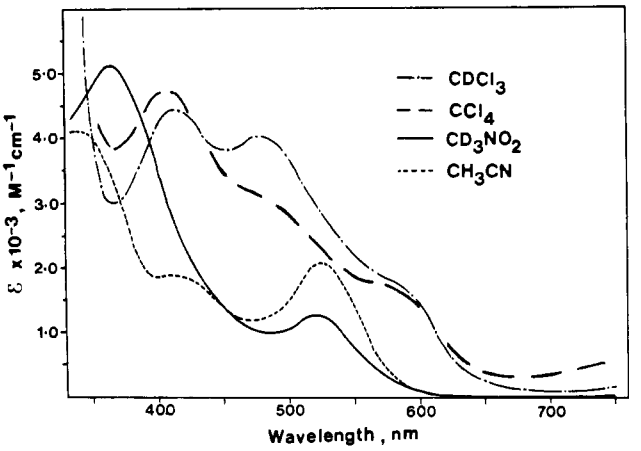

Figure 3. Visible spectra of $Ru_2Cl_5(chiraphos)_2$ in $CDCl_3$ and CCl_4; invariant with time. Spectra shown of complex in CD_3NO_2 and CH_3CN are after complete loss of absorption in the near-IR region.

Disproportionation of $Ru_2Cl_5(P\text{-}P)_2$ Complexes. The loss of the absorption bands in the near-IR spectra for $Ru_2Cl_5(P\text{-}P)_2$ (P-P = chiraphos or dppb) in CH_3CN, Me_2SO-d_6, and CD_3NO_2 implies strongly that the complexes undergo disproportionation in these solvents (eq 2). In addition to the noted differences in visible

$$Ru_2Cl_5(P\text{-}P)_2 \rightarrow \text{'}RuCl_3(P\text{-}P)\text{'} + \text{'}RuCl_2(P\text{-}P)\text{'} \quad (2)$$

spectra (Figure 3), CH_3CN solutions of the complexes $[[Ru^{II}Ru^{III}] \simeq 2 \times 10^{-3}$ M) gave molar conductivities of $\sim 110\ \Omega^{-1}\ cm^{-2}\ mol^{-1}$, while CH_3NO_2 and Me_2SO solutions were nonconducting. The reaction of $Ru_2Cl_5(dppb)_2$ and $AgPF_6$ (2:1 mole ratio) in CH_3CN led to the isolation of $RuCl_3(dppb)$, almost certainly as the dimer (**2**) (see below), and $[Ru_2Cl_3(dppb)_2(CH_3CN)_2]^+PF_6^-$ (**3**) (eq 3).

$$2Ru_2Cl_5(dppb)_2 + Ag^+ \xrightarrow{CH_3CN} \underset{\mathbf{2}}{[RuCl_3(dppb)]_2} + \underset{\mathbf{3}}{Ru_2Cl_3(dppb)_2(CH_3CN)_2^+} + AgCl \quad (3)$$

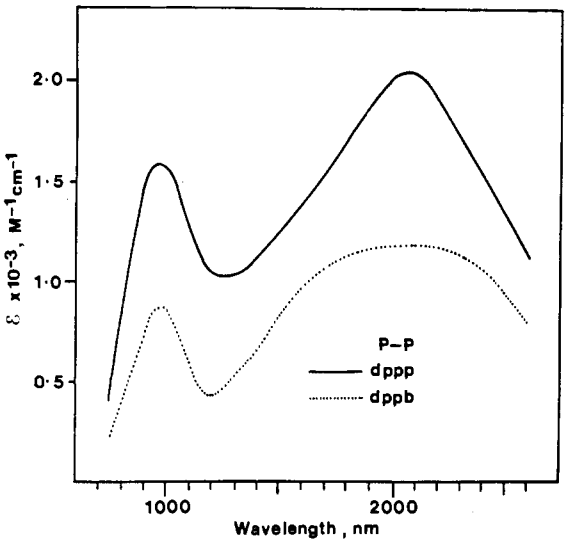

Figure 4. Near-IR spectra of $Ru_2Cl_5(dppp)_2$ and $Ru_2Cl_5(dppb)_2$ in $CDCl_3$.

Neither of the single-valence complexes **2** or **3** exhibits near-IR absorptions. Superposition of the visible spectra of the individual dimeric Ru(III) and Ru(II) complexes in CH_3CN produces a spectrum almost identical with that observed for $Ru_2Cl_5(dppb)_2$ (Figure 5), strongly supporting the suggested disproportionation of the mixed-valence complex. Since $Ru_2Cl_5(chiraphos)_2$ (**1**) in CH_3CN exhibits essentially the same visible spectrum and molar conductivity as those found for the dppb analogue, the same disproportionation (eq 2, 3) almost certainly occurs, but we have not isolated the chiraphos analogues of **2** and **3**.

In Me_2SO-d_6 and CD_3NO_2, the loss of the near-IR absorption, together with the lack of conductivity, indicates a disproportionation to the neutral Ru(III) and Ru(II) complexes (eq 2). Both products, $[RuCl_3(dppb)]_2$ (**2**) and $[RuCl_2(dppb)]_2$ (**4**), have been isolated. The maroon product (**2**) is described in the Experimental Section and is assumed to be a dimer analogous to $[RuCl_3(P\text{-}n\text{-}Bu_3)_2]_2$;[29] the color contrasts with that of the green, monomeric Ru(III) bis(phosphine) precursors used in this work. Complex **4** has been synthesized via the H_2 reduction of the mixed-valence complex $Ru_2Cl_5(dppb)_2$;[30] **4** has been detected in situ by Jung et al.,[31] and their noted ^{31}P NMR data, which demonstrate the dimeric formulation, are identical with those of our isolated species.[30] Superposition of the visible spectra of **2** and **4** in Me_2SO gives the same spectrum as that obtained for $Ru_2Cl_5(dppb)_2$ in Me_2SO (Figure 6).

Discussion

The nature of the valence state in the $Ru_2Cl_5(P\text{-}P)_2$ complexes is of fundamental importance within this new class of d^5–d^6 mixed-valence dinuclear metal complexes. The high solubility of these complexes, in particular the chiraphos derivative, permits investigation in solvents not generally associated with the study of mixed-valence complexes.[27,28]

Mixed-valence complexes frequently exhibit spectral and physical properties not shown by the single-valence congeners. The IT bands of these complexes represent a photoinduced electron transfer between metal atoms. The extent of electron delocalization between the metal centers contributes significantly to the ease of transfer and therefore has a strong influence on the physical properties. Robin and Day[32] have used the degree of delocalization as a criterion for distinguishing three broad classes of mixed-valence binuclear complexes.

(29) Nicholson, J. K. *Angew. Chem., Int. Ed. Engl.* **1967**, *6*, 264.
(30) Thorburn, I. S. Ph.D. Dissertation, University of British Columbia, 1985, to be submitted for publication.
(31) Jung, C. W.; Garrou, P. E.; Hoffman, P. R.; Caulton, K. G. *Inorg. Chem.* **1984**, *23*, 726.
(32) Robin, M. B.; Day, P. *Adv. Inorg. Chem. Radiochem.* **1967**, *10*, 264.

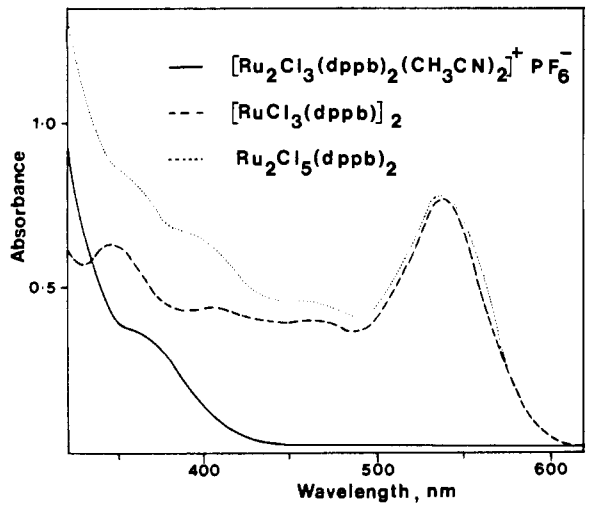

Figure 5. Visible spectra of $[RuCl_3(dppb)]_2$, $[Ru_2Cl_3(dppb)_2(CH_3CN)_2]^+PF_6^-$, and $Ru_2Cl_5(dppb)_2$ in CH_3CN. $[Ru^{III}_2] = [Ru^{II}_2] = 2.80 \times 10^{-4}$ M; $[Ru^{II}Ru^{III}] = 5.60 \times 10^{-4}$ M.

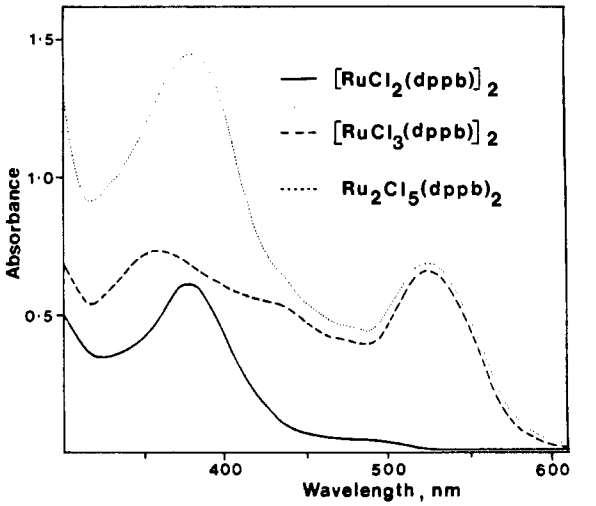

Figure 6. Visible spectra of $[RuCl_3(dppb)]_2$, $[RuCl_2(dppb)]_2$ and $Ru_2Cl_5(dppb)_2$ in Me_2SO. $[Ru^{III}_2] = [Ru^{II}_2] = 1.90 \times 10^{-4}$ M; $[Ru^{II}Ru^{III}] = 3.80 \times 10^{-4}$ M.

The X-ray structure of $Ru_2Cl_5(chiraphos)_2$ (**1**) shows the two ruthenium centers to have similar coordination geometries and metal–ligand bond distances. This clearly rules out a system containing completely localized ruthenium(II) and ruthenium(III) centers but does not distinguish between a weakly interacting system and a completely delocalized system. The solution properties of **1** are clearly solvent-dependent, with marked differences in behavior between toluene or CCl_4 and the other solvents used. Behavior in the latter cases ($CDCl_3$, $C_4H_6O_3$, DMA, Me_2SO-d_6, CD_3NO_2 (Table X)) is considered first since the solution spectra correspond to that found in the solid state. In these solvents, complex **1** exhibits a principal absorption at ca. 2340 nm, the properties of which deviate considerably from those predicted by Hush for a weakly interacting class II system.[33] The calculated bandwidth at half-height for such a system is 3140 cm^{-1}, which is approximately twice the measured value, assuming the curves to be Gaussian. In addition there is negligible variation in band energy with changing solvent. These data suggest that **1** is better formulated as a valence-delocalized class III A system.[32] This seems reasonable in view of the short metal–metal distance together with the participation of the bridging-chloride 3p orbitals, which could facilitate strong orbital interaction to produce a delocalized system. The electrochemically generated mixed-valence species $[P_3RuCl_3RuP_3]^{2+}$ (P = PEt_2Ph) exhibits a low-energy absorption at 2230 nm (ϵ = 3750 M^{-1} cm^{-1}) and was also considered to be delocalized.[34]

In toluene or CCl_4, the near-IR spectrum of **1** changes dramatically. The absence of the low-energy absorption is thought to reflect the need of a particular solvent sphere around this complex to maintain the triply chloro-bridged structure found by X-ray analysis. With the nonpolar and essentially nonsolvating toluene or CCl_4, **1** clearly changes structure. Dimerization to a tetranuclear species such as **1a** would account for several observations, and we tentatively propose such a species, which could give rise to the symmetrical absorption at 880 nm. The weaker broad absorption at lower energy (Figure 2) is attributed to remaining dinuclear species. The near-IR spectrum of **1** in toluene or CCl_4 is similar to the near-IR spectra of the dppb and diop analogues in all solvents (Table X) and implies the presence of some **1a** throughout with the larger six- and seven-membered ring systems. The spectrum of $Ru_2Cl_5(dppb)_2$ is invariant in $CDCl_3$, CCl_4, or DMA, suggesting that the larger ring size, rather than solvent, is now the major factor governing formation of **1a**. In addition, the calculated bandwidths of the high-energy band (4880 cm^{-1}) are now much greater than the measured values (3070 ± 30 cm^{-1}). On the basis of the limited data available, **1a** also appears to be delocalized. Structures akin to **1a** but with other bridging ligands (PPh_2, H, OH) have been suggested by Wilkinson's group[35] for tetrahedral Ru(II) species. The formation of **1a** from **1** would require cleavage of one of the triply bridged chloro ligands and dimerization via newly formed single chloro bridges; the formation of the Ru^{III}_2 and Ru^{II}_2 products from disproportionation also could be readily rationalized in terms of **1a** undergoing cleavage at the singly bridged chlorides.

The low solubility of $Ru_2Cl_5(dppp)_2$ prevented measurements in all solvents but $CDCl_3$, where the data are intermediate between those of the dppb and chiraphos analogues.

Acknowledgment. We thank the Natural Sciences and Engineering Research Council of Canada for financial support, Professor J. Trotter (Academic Supervisor, University of British Columbia Crystallographic Service) for the use of laboratory facilities, the University of British Columbia Computing Centre for assistance, and Johnson Matthey Ltd. for the loan of ruthenium. Dr. R. C. Thompson and J. Haynes kindly performed the Faraday measurements for us.

Registry No. **1**·$2CH_2Cl_2$, 99594-63-5; **2**, 99594-64-6; **3**, 99594-66-8; $Ru_2Cl_5(diop)_2$, 99594-67-9; $RuCl_3(P(p\text{-tolyl})_3)_2(DMA)$, 99594-68-0; $Ru_2Cl_5(dppb)_2$, 99594-69-1; $Ru_2Cl_5(dppp)_2$, 99594-70-4; $RuCl_3(PPh_3)_2(DMA)$, 99641-42-6.

Supplementary Material Available: Tables VI–IX, including calculated coordinates and temperature factors for H atoms, anisotropic thermal parameters, a complete listing of torsion angles, and observed and calculated structure factor amplitudes (46 pages). Ordering information is given on any current masthead page.

(33) Hush, N. S. *Prog. Inorg. Chem.* **1967**, *8*, 391.
(34) Heath, G. A.; Lindsay, A. J.; Stephenson, T. A.; Vattis, D. K. *J. Organomet. Chem.* **1982**, *233*, 353.
(35) Chaudret, B. N.; Cole-Hamilton, D. J.; Nohr, R. S.; Wilkinson, G. *J. Chem. Soc., Dalton Trans.* **1977**, 1546.